

Title	Performance limits of cooperative energy detection in fading environments
Authors	Horgan, Donagh;Murphy, Colin C.
Publication date	2011-10
Original Citation	Horgan, D.; Murphy, C. C. (2011) Performance limits of cooperative energy detection in fading environments . In: Simone Frattasi; Nicola Marchetti eds. 4th International Conference on Cognitive Radio and Advanced Spectrum Management (CogART) Barcelona, Spain, 26-29 Oct. 2011. ACM.
Type of publication	Conference item
Link to publisher's version	<a href="https://dl.acm.org/citation.cfm?doid=2093256.2093274-10.1145/2093256.2093274">https://dl.acm.org/citation.cfm?doid=2093256.2093274 - 10.1145/2093256.2093274</a>
Rights	ACM New York, NY, USA ©2011
Download date	2025-04-18 04:52:14
Item downloaded from	<a href="https://hdl.handle.net/10468/1041">https://hdl.handle.net/10468/1041</a>

# Performance Limits of Cooperative Energy Detection in Fading Environments

Donagh Horgan  
Department of Electrical and Electronic  
Engineering  
University College Cork  
Ireland  
donagh@rennes.ucc.ie

Colin C. Murphy  
Department of Electrical and Electronic  
Engineering  
University College Cork  
Ireland  
cmurphy@rennes.ucc.ie

## ABSTRACT

In this paper, the performance of energy detector-based spectrum sensor networks is examined under the constraints of the IEEE 802.22 draft specification. Additive white Gaussian noise (AWGN) channels are first considered, and a closed form solution for sample complexity is derived for networks of any size. Rayleigh, Nakagami and Rice fading channel models are also examined, with numerical results demonstrating the effect of these models on the required sample complexity for varying numbers of cooperating nodes.

Based on these results, the relationship between the sample complexity for AWGN, Rayleigh and Nakagami channels is examined. Through data fitting, an approximate model is derived, allowing the sample complexity for Rayleigh and Nakagami channels to be computed easily. The model is shown to be accurate across a range of practical values.

## Categories and Subject Descriptors

C.2.1 [Computer-communication networks]: Network architecture and design—*distributed networks, wireless communication*; G.3 [Probability and statistics]: Statistical computing

## General Terms

Performance, Theory

## Keywords

Cognitive radio, spectrum sensing, cooperative networks, energy detection, fading channels

## 1. INTRODUCTION

The past few decades have seen increasing utilization of the electromagnetic spectrum for a variety of applications such as radio, television, mobile telephony and wireless broadband. Typically, such services are assigned specific operating frequencies by national regulatory bodies. However,

the amount of usable bandwidth is limited, and the recent trend towards wireless ubiquity has led to a decrease in the available usable spectrum [2, 9].

Studies have shown that spectrum usage varies significantly depending on time and/or location [7]. If exploited, this variation could lead to the recovery of licensed, but unused, frequencies, paving the way for more efficient spectrum usage. The platform by which this is to be achieved is known as Cognitive Radio.

However, if the process of identifying unused frequencies, known as spectrum sensing, is not stringent enough, there is a risk of interfering with licensed signals (a television channel, for instance). This is an unacceptable situation for the licensed user, particularly if a fee has been paid for broadcast rights. Thus, spectrum sensing must be very reliable.

Cooperative spectrum sensing aims to increase the reliability of the spectrum sensing process through the sharing of information between cooperating nodes via a control channel. In energy detector-based networks, such information typically includes an estimate of the energy of the channel under investigation and, depending on the available control channel capacity, an estimate of the signal to noise ratio ( $SNR$ ) of the channel under investigation.

Soft decision fusion is an idealized view of such networks: the control channel is error-free and has infinite capacity, so both channel energy and  $SNR$  estimates can be transmitted with infinite precision; this data can then be optimally combined to reach an overall decision about the state of the channel under investigation. In this way, soft decision fusion can be viewed as an upper bound on the performance of real energy detector-based networks.

To date, soft decision networks have only been studied in cases where the number of cooperating nodes and the number of samples are small [8, 5, 6]. In this work and, to the best of the authors' knowledge, for the first time, numerical results are presented for the performance of such networks in practical operating conditions, such as those proposed in the IEEE 802.22 draft specification [12]. In such conditions, both the number of cooperating nodes and the number of samples are large. Thus, the practical performance limitations of cooperative energy detection can be ascertained.

Additionally, the performance of soft decision fusion in fading environments is examined. Again, to the best of the authors' knowledge, previous work has demonstrated the effect of fading on cooperative networks, but only in cases where the number of cooperating nodes and the number of samples are much smaller than what may be encountered in practice [3, 11]. A variety of fading channel models are considered, and numerical results, demonstrating performance limits, are presented.

## 2. SYSTEM MODEL

### 2.1 Signal model

In a network of cooperating energy detector-based spectrum sensor nodes, for a given channel, the received signal is typically represented as:

$$r_i(t) = \begin{cases} n_i(t) & H_0 \\ s_i(t) + n_i(t) & H_1, \end{cases} \quad (1)$$

where  $r_i(t)$  is the received signal at the  $i^{\text{th}}$  node,  $n_i(t)$  is the time-varying noise interference at the  $i^{\text{th}}$  node,  $s_i(t)$  is the transmitted signal at the  $i^{\text{th}}$  node and  $H_0$  and  $H_1$  are the null and alternative hypotheses, respectively.

### 2.2 Energy detection

At each energy detector, a test statistic is computed from discrete samples of the channel under investigation:

$$Y_i = \sum_{n=1}^{M_i} |r_i[n]|^2, \quad (2)$$

where  $Y_i$  is the test statistic at the  $i^{\text{th}}$  node in the network (i.e. the band energy assuming a  $1\Omega$  reference resistor),  $M_i$  is the number of samples at the  $i^{\text{th}}$  node and  $r_i[n] = r_i(nT_s)$ , where  $T_s$  is the sample period.

Without loss of generality, let it be assumed that the noise power at each node is normally distributed with zero mean and unity variance. This is equivalent to the received signal  $r_i(t)$  being normalized with respect to the noise power. While it can be argued that the estimate of this noise power is subject to uncertainty [13], for the purposes of this work, it is assumed that such uncertainties are negligible.

From (2), the distribution of the energy of the received signal at node  $i$  will be:

$$Y_i \sim \begin{cases} \chi_{2u_i}^2 & H_0 \\ \chi_{2u_i}^2(2\gamma_i) & H_1, \end{cases} \quad (3)$$

where  $\chi_{2u_i}^2$  and  $\chi_{2u_i}^2(2\gamma_i)$  are the central and noncentral chi square distributions, respectively,  $u_i = \frac{M_i}{2}$  is the time-bandwidth product at the  $i^{\text{th}}$  node and  $\gamma_i$  is the noncentrality parameter at the  $i^{\text{th}}$  node, equal to the signal to noise ratio at the  $i^{\text{th}}$  node [14; 10, p. 45-47].

It is assumed that the number of samples is equal at each node. Thus,  $M_i = M \forall i$  and  $u_i = u \forall i$ , where  $M$  is the number of samples at every node and  $u$  is the common time-bandwidth product. It is also assumed that the  $SNR$  at every node is equal, i.e.  $\gamma_i = \gamma \forall i$ . This is not a generally applicable assumption, but is allowable here as this work is concerned only with the worst case  $SNR$  limits, as specified in IEEE 802.22, i.e.  $SNR = -21dB$  [12].

It has been shown that, at low  $SNR$ , the number of samples required to reliably detect a signal becomes large [13]. Thus, invoking the central limit theorem, the test statistic becomes approximately normally distributed:

$$Y_i \sim \begin{cases} \mathcal{N}(M, 2M) & H_0 \\ \mathcal{N}(M(1+\gamma), 2M(1+\gamma)^2) & H_1. \end{cases} \quad (4)$$

### 2.3 Cooperative networks

After each detector has estimated the energy of the band under investigation, the test statistics are transmitted across a control channel to a designated master node or a fixed control center, called the fusion center, where they are summed together according to:

$$Y = \sum_{i=1}^N Y_i, \quad (5)$$

where  $Y$  is the network test statistic.

As the sum of normal random variables is also a normal random variable [4, p. 362],  $Y$  is normally distributed:

$$Y \sim \begin{cases} \mathcal{N}(MN, 2MN) & H_0 \\ \mathcal{N}(MN(1+\gamma), 2MN(1+\gamma)^2) & H_1. \end{cases} \quad (6)$$

The fusion center makes its decision by comparing the network test statistic to a threshold:

$$D \sim \begin{cases} H_0 & Y \leq T \\ H_1 & Y > T, \end{cases} \quad (7)$$

where  $D$  is the fusion center decision and  $T$  is the threshold to which the test statistic is compared. Thus, the fusion center decision probabilities are defined as:

$$Q_f = Q\left(\frac{T - MN}{\sqrt{2MN}}\right), \quad (8)$$

$$Q_m = 1 - Q\left(\frac{T - MN(1+\gamma)}{\sqrt{2MN(1+\gamma)^2}}\right), \quad (9)$$

where  $Q_f$  and  $Q_m$  are the probabilities of false alarm and missed detection, respectively, at the fusion center, and  $Q(\cdot)$  is the Q function, equivalent to the standard Gaussian complementary cumulative distribution function.

Using (8), the threshold  $T$  can be expressed as:

$$T = \sqrt{2MN}Q^{-1}(Q_f) + MN, \quad (10)$$

where  $Q^{-1}(\cdot)$  is the inverse Q function. Thus, for a given value of  $Q_f$ ,  $Q_m$  can be calculated using:

$$Q_m = 1 - Q\left(\frac{Q^{-1}(Q_f) - \sqrt{\frac{MN}{2}}\gamma}{(1+\gamma)}\right). \quad (11)$$

Rearranging (11), and using the approximation  $1+\gamma \approx 1$ , the sample complexity for AWGN channels can be determined:

$$M_0 = \frac{2}{N} \left( \frac{Q^{-1}(Q_f) - Q^{-1}(1 - Q_m)}{\gamma} \right)^2, \quad (12)$$

where  $M_0$  is the sample complexity for an AWGN channel, i.e. the number of samples required per node to reliably sense a channel at a given  $SNR$ . This equation is analogous to the sample complexity for a single energy detector derived by Tandra and Sahai [13].

From (12), it can be seen that the AWGN channel sample complexity is inversely proportional to the size of the network, i.e. increasing cooperation decreases the number of samples required to reliably sense a channel at a given  $SNR$ .

## 2.4 Fading channels

In practical situations, the received signal at the local node will be subject to fading due to the presence of scatterers in the propagation channel. In such cases, the average the probability of missed detection can be found by integrating (11) over the probability density function (PDF) of the sum of the  $SNR$  at each local node:

$$Q_{m_{avg}} = \int_0^{\infty} Q_m(x) f(N, x, \bar{\gamma}) dx, \quad (13)$$

where  $f(N, x, \bar{\gamma})$  is the PDF of the sum of the  $SNR$  at each node,  $x$  is the variable of integration representing the sum of the  $SNR$  at each node and  $\bar{\gamma}$  is the average  $SNR$  at every node [3, 11]. It should be noted here that, as  $Q_f$  does not depend on the local  $SNR$ ,  $Q_{f_{avg}} = Q_f$ , i.e. the probability of false alarm is unaffected by fading.

### 2.4.1 Rayleigh fading

The Rayleigh fading model is used to analyze ionospheric, tropospheric and urban multipath channel effects. Under this model, the attenuation of the signal is Rayleigh distributed, and so the  $SNR$  at every node becomes exponentially distributed<sup>1</sup> [10, p. 847]. The PDF of the sum of  $N$  exponential random variables  $f_{Ray}(N, x, \bar{\gamma})$  is given by [11]:

$$f_{Ray}(N, x, \bar{\gamma}) = \frac{x^{N-1} e^{-\frac{x}{\bar{\gamma}}}}{\Gamma(N) \bar{\gamma}^N}. \quad (14)$$

The average probability of missed detection for a Rayleigh fading channel can now be evaluated by substituting (14) into (13) and evaluating numerically.

### 2.4.2 Nakagami- $m$ fading

The Nakagami- $m$  fading model has been shown to be the best model for signals in urban multipath environments [10, p. 841]. Under this model, the PDF of the sum of the  $SNR$  at each node  $f_{Nak}(N, x, \bar{\gamma})$  follows a Gamma distribution:

$$f_{Nak}(N, x, \bar{\gamma}) = \left(\frac{m}{\bar{\gamma}}\right)^{mN} \frac{x^{mN-1} e^{-\frac{mx}{\bar{\gamma}}}}{\Gamma(mN)}, \quad (15)$$

where  $m$  is the Nakagami parameter, indicating fading severity. When  $m = 1$  it is equivalent to the Rayleigh channel, while  $m < 1$  indicates more severe fading and  $m > 1$  indicates less severe fading [11]. The average probability of missed detection can be evaluated using (13), as before.

<sup>1</sup>Earlier, it was assumed that the  $SNR$  at every node was equal. The proposition of a distribution of  $SNR$  values at each node does not violate this assumption as the distribution function is the same at each node and all nodes have the same average  $SNR$  value.

### 2.4.3 Rice fading

The Rice fading model is used to model situations where one path has a much stronger signal than the others, typically when a receiver has line of sight to a transmitter [10, p. 841]. To the best of the authors' knowledge, there is no closed form solution for the PDF of the sum of the  $SNR$  at each node under Rice fading. However, it is possible to calculate the PDF numerically [4, p. 362] using:

$$f_{Rice}(N, x, \bar{\gamma}) = \mathcal{F}^{-1}(\mathcal{F}(f_{Rice}(1, x, \bar{\gamma}))^N), \quad (16)$$

where  $\mathcal{F}$  represents the Fourier transform,  $\mathcal{F}^{-1}$  represents the inverse Fourier transform,  $f_{Rice}(N, x, \bar{\gamma})$  is the PDF of the sum of the  $SNR$  at each node and  $f_{Rice}(1, x, \bar{\gamma})$  is the PDF of the  $SNR$  at a single node, given by:

$$f_{Rice}(1, x, \bar{\gamma}) = \frac{K+1}{\bar{\gamma}} e^{-K - \frac{(K+1)x}{\bar{\gamma}}} I_0 \left( 2\sqrt{\frac{K(K+1)x}{\bar{\gamma}}} \right), \quad (17)$$

where  $K$  is the Rice factor, i.e. the ratio of the power of the strongest path to that of the other paths, and  $I_0$  is the  $0^{th}$  order modified Bessel function of the first kind [1]. When  $K = 0$ , the Rice channel is equivalent to the Rayleigh channel. Again, the average probability of missed detection can be evaluated using (13).

## 3. PERFORMANCE LIMITS

The IEEE 802.22 draft specification states that the probabilities of missed detection and false alarm at  $SNR = -21dB$  must be less than or equal to 10%, i.e.  $Q_{m_{avg}} \leq 0.1$  and  $Q_{f_{avg}} \leq 0.1$  [12]. Using (13), it is possible to numerically evaluate the sample complexity under such constraints. Figure 1 shows the variation of sample complexity with network size for the various channel types. As expected, the AWGN channel sample complexity is inversely proportional to the network size while, for each of the fading channels, it can be seen that, as the network size increases, the degradation in receiver sensitivity decreases, i.e. cooperation can overcome the effect of fading.

As can be seen, the Rice fading channel, with  $K = 5$ , has a sample complexity close to that of the AWGN channel, which is to be expected as the Rice channel models situations where the receiver has a line of sight to the transmitter. The Nakagami-2 channel, i.e.  $m = 2$ , also has a sample complexity close to that of the the AWGN channel, while the Rayleigh (equivalent to  $m = 1$  and  $K = 0$ ) and Nakagami-0.5 channels highlight the effect of increasing fading severity.

Of particular interest is the number of nodes it takes to achieve a sample complexity close to that of the AWGN channel. Figure 2 shows the variation of normalized sample complexity  $M/M_0$ , i.e. the ratio of fading channel sample complexity to AWGN sample complexity, for various network sizes. As can be seen, for heavily faded Nakagami channels, e.g.  $m = 0.5$ , networks with around fifty nodes should be sufficient to achieve a sample complexity close to that of AWGN. When the fading is not as severe, e.g.  $m = 1$  (equivalent to a Rayleigh channel), approximately twenty nodes are required, while in very lightly faded Nakagami channels, e.g.  $m = 2$ , as few as ten nodes are required. As Nakagami channels are primarily used to model urban envi-

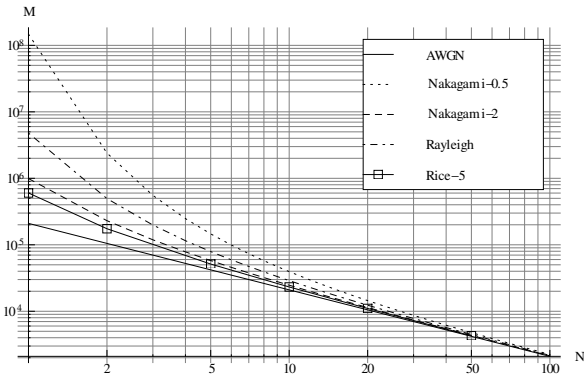


**Figure 1: Log-log plot of sample complexity against network size for  $SNR = -21dB$ ,  $Q_{m_{avg}} = 0.1$ ,  $Q_f \leq 0.1$ .**

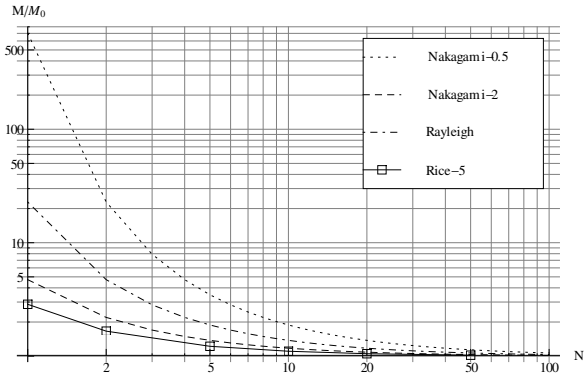


**Figure 2: Log-log plot of normalized sample complexity against network size for  $SNR = -21dB$ ,  $Q_{m_{avg}} = 0.1$ ,  $Q_f \leq 0.1$ .**

ronments, where the population density is high, it is likely that such numbers of nodes will be available.

Rice fading models situations where the receiver has a line of sight to the transmitter. Such scenarios can occur in less populated or rural environments, where there is a lower likelihood of large numbers of nodes being available for cooperation. However, as can be seen in Figure 2, as few as five nodes are required for the sample complexity to be very close to that of AWGN for the Rice channel with  $K = 5$ . The worst case Rice channel occurs when there is no line of sight, i.e.  $K = 0$ , and is equivalent to the Rayleigh fading channel. Thus, at worst, twenty nodes will be required to achieve a sample complexity close to that of AWGN.

## 4. SAMPLE COMPLEXITY MODELS

The results shown in Figure 1 are useful for determining the sample complexity required for a given network size, but only under the specified constraints. Thus, a generalized model of sample complexity is desirable. However, it is not possible to average the AWGN channel sample complexity in a similar fashion to (13) as the integral is not valid at  $x = 0$ . Thus, it is proposed that the sample complexity be approximated.

### 4.1 Rayleigh fading

For Rayleigh faded channels, the following model is proposed:

$$\hat{M}_{Ray} = \left( ae^{\frac{b}{n}} + \gamma \left( c + \frac{d}{n^e} \right) + f + \frac{g}{n^h} \right) M_0, \quad (18)$$

where  $\hat{M}_{Ray}$  is the approximate sample complexity for a Rayleigh faded channel,  $a = 1.13257$ ,  $b = 2.89472$ ,  $c = 1.26362$ ,  $d = 1.07861$ ,  $e = 13660.7$ ,  $f = -0.133695$ ,  $g = 2.66148$  and  $h = 5.28098$ .

The accuracy of the model can be verified by examining the residual<sup>2</sup>,  $M_{Ray} - \hat{M}_{Ray}$ . As can be seen in Table 1, the mean of the absolute value of the residuals is less than four samples with a standard deviation of fewer than five samples, while the average absolute percentage error,  $100 \times \frac{|M_{Ray} - \hat{M}_{Ray}|}{M_{Ray}}$ , is 0.9% with a standard deviation of 1.23%.

The five largest residual and percentage error values are shown in top and bottom halves of Table 2, respectively. As can be seen, the largest residuals occur where the percentage errors are small and the largest percentage errors occur when the residuals are small.

### 4.2 Nakagami fading

For Nakagami faded channels, the following model is proposed:

$$\hat{M}_{Nak} = \left( ae^{\frac{b}{mn}} + \gamma \left( c + \frac{d}{(mn)^e} \right) + f + \frac{g}{(mn)^h} \right) M_0, \quad (19)$$

where  $\hat{M}_{Nak}$  is the approximate sample complexity for a Nakagami faded channel,  $a = 0.953638$ ,  $b = 3.16447$ ,  $c = 1.39815$ ,  $d = 0.679112$ ,  $e = 3.59613$ ,  $f = 0.0973942$ ,  $g = 0.322522$  and  $h = 9.07618$ .

As can be seen in Table 1, the mean of the absolute value of the residuals<sup>3</sup> is less than eighty three samples with a standard deviation of fewer than two hundred and eighteen samples, while the average absolute percentage error is 2.911% with a standard deviation of 2.961%.

The five largest residual and percentage error values are shown in top and bottom halves of Table 3, respectively. As can be seen, again, the largest residuals occur where the percentage errors are small and the largest percentage errors occur when the residuals are small.

### 4.3 Rice fading

For Rice faded channels, a sufficiently accurate approximation could not be found due to the non-linear variation of  $M_{Rice}$  with  $K$ . However, at worst ( $K = 0$ ), Rice fading is equivalent to Rayleigh fading and, at best ( $K \rightarrow \infty$ ), it is equivalent to AWGN. Thus,  $1 \leq M_{Rice} \leq M_{Ray}$ .

<sup>2</sup> $M_{Ray}$  was calculated numerically using (13) for each unique pair  $\{N, SNR\}$  in the sets  $N \in \{1, 2, 3, 4, 5, 10, 20, 50\}$  and  $SNR \in [-21dB, 0dB]$  (in 1dB intervals).

<sup>3</sup> $M_{Nak}$  was calculated in a similar fashion to  $M_{Ray}$  for each unique triplet  $\{N, SNR, m\}$  in the sets  $N \in \{1, 2, 3, 4, 5, 10, 20, 50\}$ ,  $SNR \in [-21dB, 0dB]$  (in 1dB intervals) and  $m \in \{0.5, 0.75, 1, 1.25, 1.5, 1.75, 2\}$ .

**Table 1: Residual statistics for the approximate channel models.**

Channel type	Rayleigh	Nakagami
Mean absolute residual	3.737	82.369
Standard deviation	4.171	217.777
Mean absolute percentage error	0.9%	2.911%
Standard deviation	1.23%	2.961%

**Table 2: Largest residuals and percentage errors (PE) for the approximate Rayleigh channel model.**

$N$	$SNR$	$M_{Ray}$	Residual	PE
2	-17dB	78821.9	17.443	0.022%
2	-21dB	495625	-17.334	-0.004%
2	-16dB	49807	16.758	0.034%
2	-18dB	124777	16.462	0.013%
5	-21dB	79045.1	16.041	0.020%
2	0dB	42.197	2.688	6.371%
3	0dB	19.071	1.068	5.602%
4	0dB	11.958	0.570	4.765%
2	-1dB	62.724	2.814	4.486%
5	0dB	8.633	0.352	4.077%

**Table 3: Largest residuals and percentage errors (PE) for the approximate Nakagami channel model.**

$N$	$SNR$	$m$	$M_{Nak}$	Residual	PE
1	-21dB	1.25	$2.52 \times 10^6$	-3452.3	-0.137%
1	-21dB	2	991250	2162.29	0.218%
1	-20dB	1.25	$1.59 \times 10^6$	-2138.19	-0.134%
1	-21dB	1	$4.79 \times 10^6$	1353.32	0.028%
1	-20dB	2	625805	1339.53	0.214%
50	-3dB	2	1.674	-0.191	-11.391%
50	-3dB	1.75	1.680	-0.190	-11.305%
50	-4dB	2	2.443	-0.274	-11.209%
50	-3dB	1.5	1.687	-0.189	-11.191%
50	-4dB	1.75	2.451	-0.273	-11.123%

## 5. CONCLUSION

An expression for the sample complexity of cooperative energy detector-based networks operating on AWGN channels was derived and shown to be inversely proportional to network size. Numerically generated sample complexity data were presented for a variety of fading environments. In all cases, it was demonstrated that sample complexity decreases as cooperation increases and that the number of nodes required to overcome multipath effects is realistic.

Through data fitting, sample complexity models were derived for cooperative networks operating on Rayleigh and Nakagami faded channels with the constraint  $Q_{m_{avg}} = 0.1$ ,  $Q_f \leq 0.1$ . These models were shown to be highly accurate

across a range of practical  $SNR$  values and network sizes. For Rice channels, it was noted that sample complexity is upper bounded by Rayleigh channel sample complexity and lower bounded by the AWGN channel sample complexity.

As soft decision type networks were considered, the results presented here provide an upper bound for the performance of real energy detector-based networks, which have non-idealities such as finite control channel capacity, requiring the quantisation of local sensing data, parameter estimate uncertainties, and transmission errors in the control channel. The incorporation of such factors into these models is expected to be the focus of future work.

## 6. REFERENCES

- [1] F. F. Digham, M. S. Alouini, and M. K. Simon. On the energy detection of unknown signals over fading channels. In *Communications, 2003. ICC'03. IEEE International Conference on*, volume 5, page 3575–3579, 2003.
- [2] FCC. FCC spectrum inventory table, 1996.
- [3] A. Ghasemi and E. S. Sousa. Opportunistic spectrum access in fading channels through collaborative sensing. *Journal of Communications*, 2(2):71–82, 2007.
- [4] A. Leon-Garcia. *Probability, statistics, and random processes for electrical engineering*. Pearson/Prentice Hall, 2008.
- [5] J. Ma and Y. Li. Soft combination and detection for cooperative spectrum sensing in cognitive radio networks. In *Global Telecommunications Conference, 2007. GLOBECOM '07. IEEE*, pages 3139–3143, 2007.
- [6] J. Ma, G. Zhao, and Y. Li. Soft combination and detection for cooperative spectrum sensing in cognitive radio networks. *Wireless Communications, IEEE Transactions on*, 7(11):4502–4507, 2008.
- [7] M. A. McHenry and K. Steadman. Spectrum occupancy measurements, location 1 of 6: Riverbend park, great falls, virginia, tech. rep. Technical Report 1, The University of Kansas Center for Research, Inc., Riverbend Park, Great Falls, Virginia, Apr. 2004.
- [8] R. Niu, B. Chen, and P. K. Varshney. Fusion of decisions transmitted over rayleigh fading channels in wireless sensor networks. *Signal Processing, IEEE Transactions on*, 54(3):1018–1027, 2006.
- [9] NTIA. NTIA frequency allocation chart, 2003.
- [10] J. G. Proakis and S. Masoud. *Digital Communications*. McGraw-Hill Higher Education, Boston, 5th edition, 2008.
- [11] B. Shahid and J. Kamruzzaman. Weighted soft decision for cooperative sensing in cognitive radio networks. In *Networks, 2008. ICON 2008. 16th IEEE International Conference on*, page 1–6, 2010.
- [12] S. Shellhammer. Spectrum sensing in IEEE 802.22. Santorini, Greece, June 2008. EURASIP.
- [13] R. Tandra and A. Sahai. SNR walls for signal detection. *Selected Topics in Signal Processing, IEEE Journal of*, 2(1):4–17, 2008.
- [14] H. Urkowitz. Energy detection of unknown deterministic signals. *Proceedings of the IEEE*, 55(4):523–531, 1967.